Title: Porosity and density measurements of sodium acetate trihydrate for thermal energy storage

Authors: Mark Dannemand[1,4]*, Monica Delgado[4], Ana Lazaro[4], Conchita Peñalosa[4], Carsten Gundlach[2], Camilla Trinderup[3], Jakob Berg Johansen[1], Christoph Moser[5], Hermann Schranszhofer[5], Simon Furbo[1]

[1] DTU Civil Engineering, Technical University of Denmark, Brovej, Building 118, DK-2800, Kgs. Lyngby, Denmark

[2]DTU Physics, Technical University of Denmark, Fysikvej, Building 311, 2800, Kgs. Lyngby, Denmark

[3]DTU Compute, Technical University of Denmark, Richard Petersens Plads, building 324, DK-2800, Kgs. Lyngby, Denmark

[4]Aragón Institute for Engineering Research (I3A), Thermal Engineering and Energy Systems Group,

University of Zaragoza, Agustín Betancourt Building, C/María de Luna 3, 50018 Zaragoza, Spain

[5]Graz University of Technology, Institute of Thermal Engineering, Inffeldgasse 25/B, 8010 Graz, Austria

[*]*Corresponding email: markd@byg.dtu.dk*

Abstract:

Sodium acetate trihydrate (SAT) can be used as phase change material in latent heat storage with or without utilizing supercooling. The change of density between liquid to solid state leads to formation of cavities inside the bulk SAT during solidification. Samples of SAT which had solidified from supercooled state at ambient temperature and samples which had solidified with a minimal degree supercooled were investigated. The temperature dependent densities of liquid and the two types of solid SAT were measured with a density meter and a thermomechanical analyzer. The cavities formed inside samples of solid SAT, which had solidified after a high or minimal degree of supercooling, were investigated by X-ray scanning and computer tomography. The apparent density of solid SAT depended on whether it solidified from a supercooled state or not. A sample which solidified from a supercooled liquid contained 15% cavities and had a density of 1.26 g/cm^3 at 25 °C. SAT which had solidified with minimal supercooling contained 9% cavities and had a density of 1.34 g/cm^3 at 25 °C. The apparent densities of the solid SAT samples were significant lower than the value of solid SAT reported in literature of 1.45 g/cm^3. The density of liquid and supercooled SAT with extra water was also determined at different temperatures.

Keywords: Sodium acetate trihydrate; density; phase change material; x-ray tomography; thermal energy storage; cavity

1. Introduction

Thermal energy storage is needed to match the varying supply of renewable energy sources such as solar energy with the more predictable demand for heating of buildings. A lot of research focuses on phase

change materials (PCM) because they allow for denser heat storage compared to a sensible heat storage with e.g. water as the storage medium. The ability of the PCM to remain at the melting point for an extended period during charge and discharge while absorbing or releasing thermal energy allows for favorable operating conditions for some applications. Especially in some applications where the melting temperature of the PCM fits the supply and demand temperatures.

Sodium acetate trihydrate (SAT) was identified as a heat storage material with high potential [1–8]. SAT has a relatively high melting enthalpy or latent heat of fusion compared to other PCMs and a melting point of approximately 58 °C. In addition, the thermal conductivity of salt hydrates is generally higher than e.g. paraffins [9]. These characteristics fit well with space heating requirements and domestic hot water preparation [10]. This temperature level is also easily reached by simple solar thermal collectors and potentially by heat pumps. Stability of the SAT composite in repeated thermal cycles needs to be confirmed with boundaries representing the intended application.

1.1. Supercooling

The material SAT itself has the ability to supercool far below its melting point. In most applications, the supercooling has been seen as a problem. This has been avoided by adding nucleation agents to the SAT mixture to start solidification with minimal supercooling during discharge [2][11,12]. Several researchers look into developing PCM composites of SAT with thickening agents and nucleation agents for improving the PCMs performance in systems where supercooling is suppressed [13–15]. On the other hand, actively utilizing the supercooling gives the possibility to store energy over long periods without thermal loss in part of the storage period. This is done by having the melted SAT remain in supercooled state in the storage period at ambient temperature so that the latent heat of fusion can be stored long term [4,8].

1.2. Material properties

SAT, with the chemical notation $NaCH_3COO{\cdot}3H_2O$, consists of 60.3 % sodium acetate and 39.7% water. SAT is considered an incongruently melting salt hydrate, which suffers from phase separation. The problem of phase separation has been sought solved by adding thickeners or extra water to the SAT [7,8,16–20]. The key properties, which determine the capacity of a PCM heat storage, are the specific heat capacity in solid and liquid phase, latent heat and the density of the PCM. These thermophysical properties are important to know when designing and sizing a storage. Ma et al. did a study on SAT for seasonal heat storage which include listing thermo-physical properties of SAT and aqueous solution of sodium acetate [21].

Kousksou et al. did a review article on applications and challenges of energy storage and touched on latent heat storage [6]. They mention that despite the fact that PCMs are extensively researched, their thermophysical properties are lacking in the literature. Kenisarin and Mahkamov summaries the material properties of different salt hydrates including SAT in a review article [9]. They indicate that the values of the thermophysical properties of SAT measured by different researchers have significant variations. Typical values in the literature for densities of SAT are 1.45 g/cm^3 for solid phase and 1.28 g/cm^3 for the liquid phase with no dependence on temperature or thermal expansion coefficients provided [22]. Noting that the density of the solid SAT of 1.45 g/cm^3 is for a SAT crystal formed with a cooling rate low enough to have the crystallization process occur slowly and form a dense crystal. Only Inaba et al. present results of temperature dependent densities of solid and liquid SAT [23]. In that study, the presented equation giving

the density of liquid SAT as a function of the temperature does however not match with the diagram shown in the article. The same faulty expression is listed by Kenisarin and Mahkamov [9].

The effective density of SAT, may in the case, where it has solidified from supercooled state be very much like the density of the liquid SAT because it will solidify rapidly without time to contract to a dense mass. Therefore, a volume of cavities representing the difference in liquid and solid density may be enclosed in the solidified SAT.

1.3. Limitations

One of the limitations of using PCMs as heat storage material is a low heat transfer to and from the PCM (especially in solid state). The heat transfer is affected by the heat exchanger design and the properties of the PCM. The thermal conductivity governs the heat transfer when the PCM is in solid phase. In liquid state convection and thermal conduction governs the heat transfer. As most other PCMs, SAT has a relatively low thermal conductivity. The values in the literature for thermal conductivity of solid SAT varies between 0.4-0.7 W/(m·K) [9].

Dannemand et al. reported that the crystal structure of SAT which had solidified from a supercooled state was different from SAT which had solidified with minimal supercooling [19]. They state that the SAT solidified from a supercooled state did not contract uniformly and cavities were formed in the PCM during the fast solidification and crystallization. They showed that the measured thermal conductivity was lower in a sample which had solidified from supercooled state (0.3-0.6 W/(m·K)) compared to a sample which had solidified with minimal supercooling (0.7 W/(m·K)).

1.4. Heat storage applications

Various PCMs have been applied in heat storage development. Khan et al. did a review on ways to enhance the performance of PCMs in heat storages [24]. Dheep and Sreekumar did a review on the influence of nanoparticles on properties of different PCMs [25]. Sharif et al. describes ways to integrate PCM into domestic hot water storage systems (DHW) and concludes that PCM thermal energy storage is expected to lower cost and the volumes of heating and DHW systems [26]. Xu et al. did a review article on seasonal heat storage for solar heating system and mention SAT with supercooling as one of the technologies [27]. Zhou and Han did a numerical simulation of supercooled SAT in heat storage application [28]. Aydin et al. concluded that latent heat storage can improve the performance of solar heating systems and are especially useful during autumn and spring in the Istanbul climate [29]. Fazilati and Alemrajabi investigated adding PCM to a water tank for the solar heating system and find that the PCM improves its performance [30]. Sharma et al. also did an extensive review on thermal storage applications with PCM and state that the high storage density and isothermal storage process makes PCMs effective storage materials [7]. Cabeza et al. did a review on PCMs in building applications and presents different ways of applying the materials [22]. They present an overview of a range of PCMs, list important characteristics of PCMs, which has to be considered when designing an application. They also show different ways of encapsulating PCMs. Also a group of researchers in the International Energy Agency Solar Heating and Cooling program have in Task 32 and Task 42 investigated material properties and applications with PCMs including SAT [31], [32].

When applying SAT or any other PCM in a heat storage it must be considered how the material will act in bulk quantities. It may be that the dimensions of the storage, operating temperature, repeated cycling etc. may cause the PCM to act differently compared to investigations made on small samples. Also, whether the

storage is intended to operate with supercooling or not must be considered as it affects the thermal conductivity of the solid SAT.

In a heat storage design, the change of density between solid and liquid states and the associated volume change has to be accommodated for in some way. In experimental investigations Dannemand et al. solved the expansion and contraction of SAT inside prototype heat storage units by integrating an expansion tank in the storage design [16,17]. This allowed for operating the storage units without pressure built up and associated deformations of the storage tank.

Studies have suggested to use oil with high thermal conductivity as an additive to the PCM to fill in the cavities formed during contraction of the PCM. This should enhance heat transfer in the PCM and between PCM and heat exchanger [17]. Oil can also be used as a heat transfer fluid by letting it be in direct contact with the PCM [33],[34],[35]. Oil does not mix with water or SAT and will float on top of the liquid state SAT. With these heat transfer enhancement methods in mind, it is relevant to investigate how cavities are formed inside SAT during solidification. The cavities may be enclosed in the PCM, or the cavities may form channels through the PCM, where the oil can flow. This will affect the heat transfer characteristics of the PCM-oil mixture.

1.5. Scope

The temperature range that is relevant to investigate considering heat storage systems for solar heating system, for space heating and domestic hot water preparation is considered to be 10-90 °C. The density in solid and liquid state are therefore investigated in this temperature range.

When designing a storage tank for a SAT, it is important to know how the density changes between the solid and liquid state SAT, so the expansion and contraction can be handled in a way that does not reduce the performance of the storage unit. Cavities formed inside the PCM during fast solidification may reduce the apparent density of the solid SAT.

The temperature dependent density of solid SAT formed from crystallization of supercooled SAT is presented. This distinction between solid SAT with a compact crystal structure, which is the one typically reported in the literature, and SAT solidified with or without prior supercooling has not previously been made. The temperature dependent densities of liquid SAT with different amounts of extra water are presented – something not previously reported.

The layouts of the cavities in solid SAT are investigated with the use of X-ray and Computer Tomography (CT). The cavities in two SAT samples, which had solidified after a high or a minimal degree of supercooling, were compared. This is done by evaluating the fraction of cavities in the SAT and by determining how much of the volume is enclosed cavities and how much is continuous channels. This has not been done previously.

2. Methods

2.1. Density

2.1.1. Density measurements in the solid phase

In order to obtain the density related the temperature of SAT in the solid phase, a thermomechanical analyzer (TMA) from the manufacturer Mettler Toledo, model TMA 841, was used. Traditionally, TMAs are used to characterize the linear expansion of materials. A stress is applied to the material and the resulting strain is measured while the material is subjected to a controlled temperature program. To measure this expansion, a probe is placed on the sample imposing a minimum stress, allowing the tracking of the sample in its expansion or contraction during the test, with a resolution lower than 1 nm. The sample temperature is measured very close to the sample by means of a K-type thermocouple. A thin quartz glass coating protects it against direct contact and contamination. The temperature accuracy is 0.25 °C. Before each temperature ramp, the samples were kept in isothermal state at 10 °C for 10 minutes to set the precondition for the experiment. A heating rate of 1K/min was applied. At the end of the heating, the sample was kept at a constant temperature for 10 minutes. Figure 1 shows the details of the probe and the sample support.

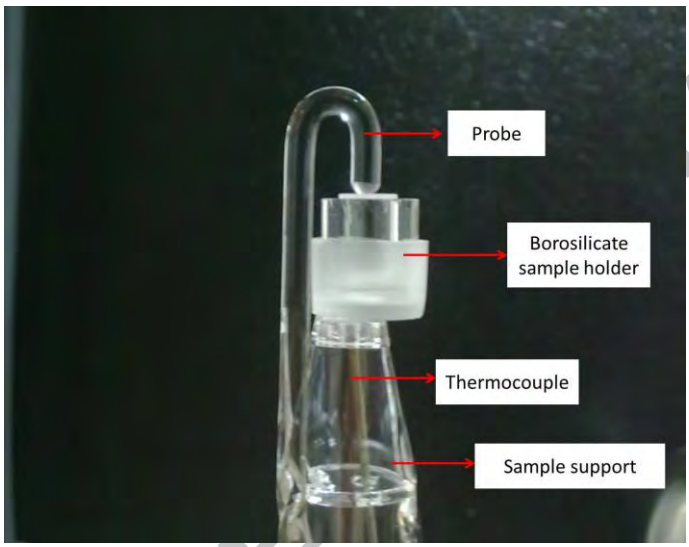

Figure 1. Details of the probe and the sample support from TMA 841.

Since the TMA provides measurements of the thermal expansion coefficient, it is necessary to determine the density at a set temperature, in this case, at room temperature. For that purpose, the sample mass was measured by a Mettler Toledo AB135-S precision scale with an accuracy of 0.01 mg, and the dimensions with a caliber, which has an accuracy of 0.0011 mm.

The solid SAT samples were prepared using two different sample holders: 1) one called as open sample holder and 2) one called as closed sample holder. ½

The measurements with the open and closed sample holders were executed with a blank correction. This blank correction consisted in carrying out a baseline measurement, with the probe supporting on the empty sample holder in the same conditions as when the sample was measured. Subtracting this signal, errors related to the thermal expansion from the support sample, probe and sample holder, were eliminated. Both the open and close sample holders were placed between the sample support and the

probe. Two identical samples for both open and closed sample holders were prepared and the resulting average values displayed in the result section.

Open samples

SAT samples were prepared in a stainless steel cylinder with a diameter of 12.06 mm and a height of 4.99 mm (see Figure 2). The samples were prepared by melting SAT in a closed glass jar in an oven at 90 °C. A seed SAT crystal was placed inside the sample holder to avoid supercooling during the cooling down. The melted SAT was poured into the sample holder. Once the SAT had cooled to ambient temperatures and solidified, the surfaces of the solid SAT sample were made level. The mass, dimensions and the thermal expansion of the sample were measured with the sample being inside the cylindrical sample holder. The thermal expansion over the temperature range 10 °C to 40 °C was measured.

As the SAT solidified and cooled down, cavities were formed in the central area of the sample, as seen in Figure 2. It was assumed that the thermal expansion was only occurring in the axial direction of the sample, as the diameter (radial direction) was kept constant by the sample holder. Thermal expansion of the sample holder may have increased its diameter, however the thermal expansion coefficient of stainless steel is significant lower than for SAT and this effect was therefore neglected.

Figure 2. Open sample holder with solid SAT, 12.06 mm diameter and 4.99.mm height.

Closed sample

Sample holders of borosilicate glass consisting of a bottom cup and a lid, especially designed by Mettler Toledo to measure liquid samples, were used to measure samples in closed sample holders (see Figure 1). The samples were prepared by pouring melted SAT into the holder. Once the SAT had cooled down a seed crystal was added to initialize the crystallization. This gave a solid SAT sample which had been crystalized from supercooled SAT at ambient temperature. Before starting the test, it was ensured that no SAT was jammed between the cup and lid so that the lid could move freely together with the sample in its contraction and expansion, transferring this movement to the probe.

The thermal expansion over the temperature range 10 °C to 80 °C was measured. Like for the stainless steel sample holder it was assumed that the thermal expansion occurred only in the axial direction of the sample as the diameter (radial direction) was kept constant by the borosilicate sample holder. When the SAT was heated over the melting temperature, the liquid SAT spilled out of the sample holder. Measurement of the SAT in liquid state with the TMA were therefore not possible with this sample holder. Force applied to the samples was 0.01 N.

When determining the volume of the sample in the borosilicate sample holder, a correction related the specific shape of the sample holder was applied. The correction was required due to the different curvatures of the transitions from the flat surfaces to the sides of the cup and lid (see Figure 3).The correction factor had previously been determined in a calibration process with water.

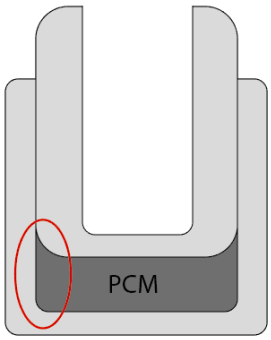

Figure 3. Diagram of borosilicate sample holder with PCM and basis for corrected volume.

In order to associate a deviation to the measurements executed, a solid octadecane sample inside the borosilicate sample holder, whose density is known [36] has been measured having adopted the same measuring procedure. The deviation observed was 1.3 %.

2.1.2. Density measurements in the liquid phase

A Mettler Toledo Density meter DM40, which measuring principle is based on the oscillating U-tube, was used to measure the density of the melted SAT (60.3 % sodium acetate and 39.7% water). The SAT was preheated in an oven to 90 °C before injected into the density meter. Successful measurements were made on SAT samples in 10 K steps from 60-90 °C. The measurements were repeated twice. Measurements in supercooled state at 50 °C and below was not possible as the SAT sample crystalized. A Mettler/PAAR DMA45 was used to measure the liquid density of SAT samples with extra water. The DMA 45 is based on the same measurement principle as the DM40 (oscillating U-tube) and was calibrated according to the manufacturer recommendation. Measurements were carried out on samples with 58/42%, 56/44%, 54/46% and 52/48 % sodium acetate/water by weight. Density measurements were successfully made on the samples with extra water down to 20 °C, hence including the supercooled state.

Before the measurements, the DM40 Density meter was adjusted at 60 °C using two standard substances whose density is known: distilled water and dry air. The ideal had been to do the adjustment at each temperature step of the temperature program: 60, 70, 80 and 90 °C, since the adjustment constants, characteristic of the measurement cell, depend on temperature. However, above 60 °C it was not possible due to the water evaporation.

Once the adjustment of the density meter was executed, and likewise with the TMA measurements, a density standard (the standard oil S3 from Paragon Scientific) was measured to associate a deviation to the SAT measurements. These measurements were executed at 60 and 80 °C, because the certificate of calibration provided certified values at these temperature steps according to ASTM D1480 and because they were within the temperatures range of the SAT test. The deviation observed was 0.68% at 60 °C and 0% at 80%.

X-ray

2.2.1. Sample preparation

Two samples of SAT were prepared in closed glass jars. The samples were heated and melted in an oven. One sample was seeded with SAT as it cooled down to ambient temperature to minimize supercooling. The other sample was let to cool down to ambient temperature before a seed SAT crystal was added to initiate the solidification. Cores from the samples were drilled out. Each sample had a diameter of 10 mm and a height of approximately 15 mm. The sample that solidified from supercooled state appeared more white and less dense in structure.

2.2.2. X-ray micro tomography measurements

The internal structure of the two samples were investigated with X-ray micro tomography using the commercial system “Zeiss Xradia 410 versa”. The system has an X-ray source in reflection geometry and operates with a pre voltage between 40 kV and 150 kV, samples can be mounted in the system allowing for 360° rotation.

The two core-samples were investigated and a large volume X-ray tomography scan was conducted using the systems Large-Field-Of-View (LFOV) objective to map the entire core-sample with a pixel size of 24.2 µm and 22.6 µm and a pre voltage of 40 kV, images were acquired in 1601 angle steps.

Tomographic data were reconstructed using the commercial software available for the system. The reconstruction software is based on the FDK method (Feldkamp algorithm) which is a filtered back projection algorithm [37].

2.2.3. Segmentation

The scanned samples were analyzed with advanced image analysis tools. The goal was to obtain a segmentation, i.e. identify voxels representing either material or air. At first, each voxel was segmented into foreground (material) or background (air) with Linear Discriminant Analysis (LDA). The LDA returns a probability for each voxel belonging to the foreground. The probability estimates were used as input to Iterated Conditional Modes (CIM). Since this method is based on Markov Random Fields it ensures that the global structure, i.e. neighborhood information, of the material is taken into account in the segmentation step. Finally, a morphological opening operation was applied to the segmentation returned by ICM, in order to separate components of the segmentation.

The segmentation was subject to a connected components analysis to identify connected voxels representing air. The fraction of air in a sample was computed as the number of voxels classified as air relative to the total number of voxels within the sample volume. The connected air components within the volume were found and used for estimating the relative ratio of encapsulated air.

3. Results and discussions

3.1. Density

3.1.1. Solid phase

The density of the solid SAT in the closed sample which had solidified from supercooled state was determined to be 1.24 - 1.28 g/cm^3. This measured solid density was up to 14.5% lower than the typical value reported in literature of 1.45 g/cm^3 for the SAT crystal. The density of the solid SAT in the open sample which had solidified with minimal supercooling was determined to be 1.33 - 1.34 g/cm^3.

Cavities were observed in the solid SAT samples. This was due to the contraction of the SAT as it cooled down and solidified during preparation of the sample. Cavities or air gaps were therefore formed in the central upper part of the samples. The density was higher in the samples made in the open stainless steel cylinder compared to the samples in the closed borosilicate sample holders. This may be due to method of preparation of the sample where the open samples were prepared with avoidance of supercooling in mind whereas the closed sample experienced supercooling down to ambient temperature before solidification.

In the open samples, an obvious cavity was observed in the upper central part. This gave an obvious error in determining the density of the solid SAT when considering the densest crystal structure of the SAT. This behavior could however be expected in an actual application with SAT where melting and solidification occurs. Reliable measurements for the open sample were achieved up to 40 °C and up to 50 °C for the closed sample. At higher temperatures, evaporation of the water from the SAT in the open sample may have been the reason for measurement uncertainties.

The measured density of liquid SAT varied from 1.29 g/cm^3 at 60 °C to 1.27 g/cm^3 at 90 °C and fitted with the typical literature value of 1.28 g/cm^3. The measured densities of SAT with extra water varied from 1.24

g/cm^3 at 80 °C to 1.28 at 20 °C for a sample with 48 % water. The determined densities of each experiment is displayed in Figure 4 along with the literature values from Lane [38] and Inaba [23]. The "SAT (s) open" samples represent the density of SAT solidified with minimal supercooling in the open sample holders. The "SAT (s) closed" samples represent the density of SAT solidified from supercooling to ambient temperature in the closed borosilicate sample holders. 39.7% represents the water content of SAT. 42%, 44%, 46%, 48% represent the water content of the liquid samples of SAT with extra water and the measured densities.

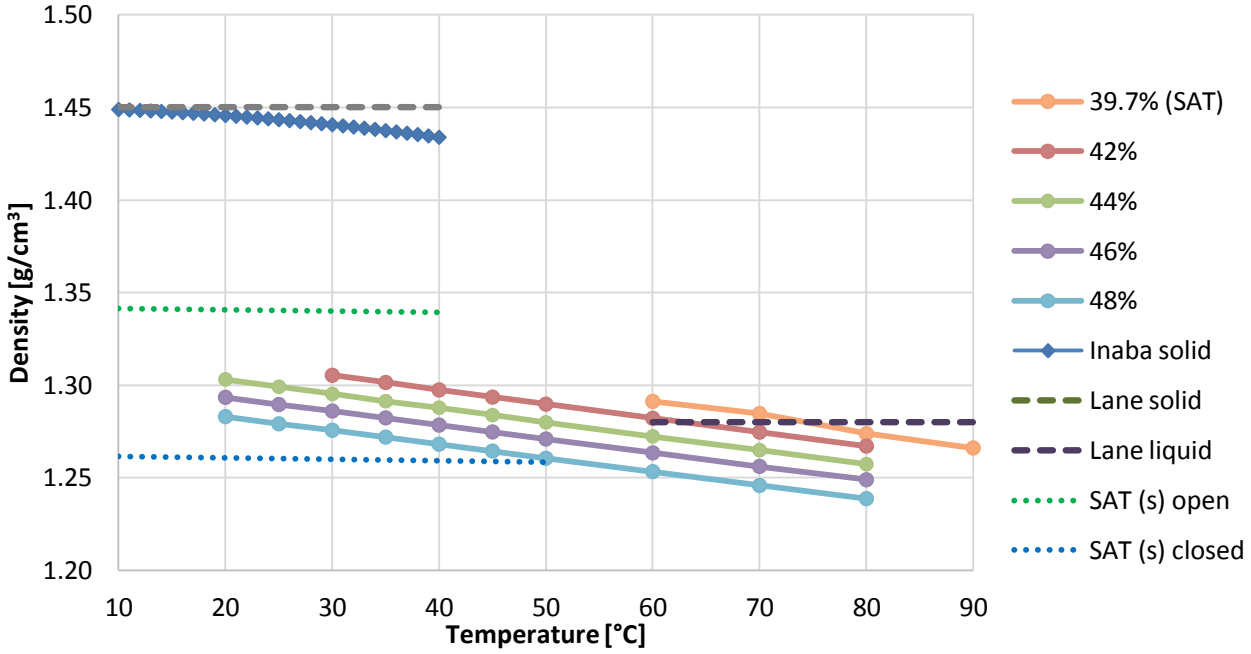

Figure 4. Density of solid and liquid SAT including SAT with extra water in supercooled state.

Equations (1, 2, 3) expressing the densities as a function of temperature for each sample type is determined based on the average of the measurements in each sample type.

The density of SAT solidified with minimal supercooling (measured in the open cylinder sample holder) as a function temperature can be expressed by (1):

$$\rho_{s(non-supercool)} = -7.800 \cdot 10^{-5} \cdot T + 1.3423 \qquad \text{For } 10\ °C \le T \le 40\ °C. \qquad (1)$$

The density of SAT solidified from supercooled state (measured in the closed borosilicate sample holder) as a function temperature can be expressed by (2):

$$\rho_{s(supercool)} = -7.600 \cdot 10^{-5} \cdot T + 1.2622 \qquad \text{For } 10\ °C \le T \le 50\ °C. \qquad (2)$$

The density of liquid SAT (measured in the Density meter) as a function temperature and water content can be expressed by (3):

$$\rho_l = -7.581 \cdot 10^{-4} \cdot T - 4.6340 \cdot 10^{-3} \cdot w + 1.5218 \qquad (3)$$

For 20 °C ≤ T ≤ 80 °C, 44 % ≤ w ≤ 48 %; 30 °C ≤ T ≤ 80 °C, w = 42 % and 60 °C ≤ T ≤ 90 °C, w = 39.7 %.

The expressions for the liquid density deviates less then +/- 0.1% and +/- 0.001 g/cm³ compared to the measurements. The expression for liquid densities determined in this study deviates less than 1% from the expression reported by Ma et al. [21].

3.2. X-ray

Cut planes and a 3D image of the scanned SAT samples are shown in Figure 5 and Figure 6. The two samples were very different in their composition.

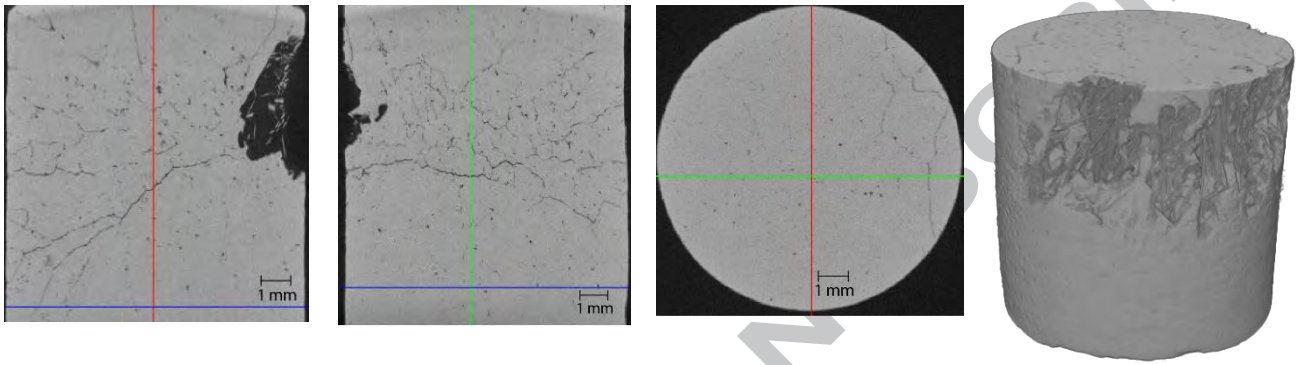

Figure 5a, b, c and d. Cut planes sliced in X-, Y- and Z-axis directions and 3D illustration of sample solidified with minimal supercooling

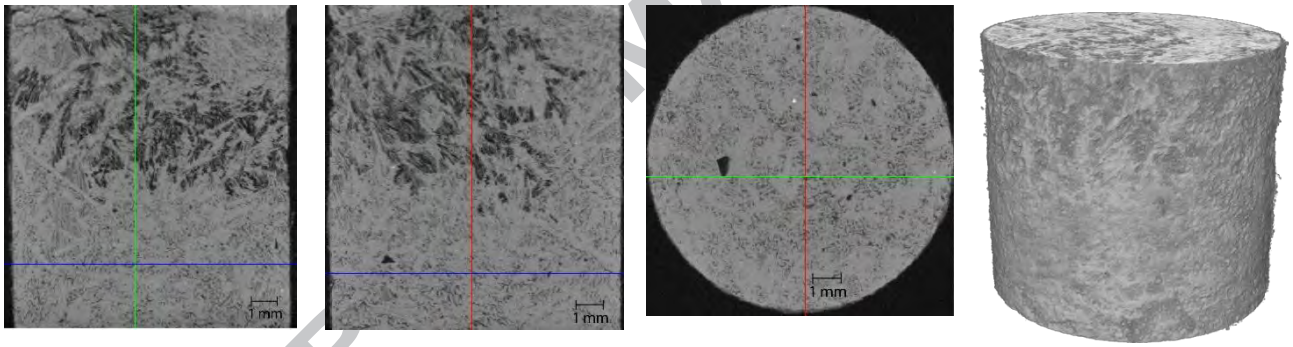

Figure 6a, b, c and d. Cut planes sliced in X-, Y- and Z-axis directions and 3D illustration of sample solidified from supercooled state

It can be seen that in the upper parts of the samples appear to be more cavities. This is especially pronounced for the sample, which had solidified from supercooled state. The phenomena may be due to how the sample cools down after crystallization and where in the sample the full phase change is completed last. In the sample, which solidified with minimal supercooling, there was one major cavity in the sample whereas in the sample, which solidified from supercooled state, cavities were dispersed over a larger volume. This corresponds well with the findings of Dannemand et al. who found that the measured thermal conductivity was lower in the upper part of a SAT sample which solidified from supercooled state compared to the lower part of the sample [19].

3.2.1 Segmentation

In the following, the center slice of the scanned part has been extracted, so that the analysis is based on slices that do not have scanning artefacts. Figure 7 and Figure 8 show the slices of the raw data and their corresponding segmentations as well as 3D illustration of both samples.

The outcome of the segmentation analysis is a volume with 551 slices with two classes representing encapsulated air and air channels attached to the surface of the sample. The red parts of the segmentation represent connected cavities and the green parts represent enclosed cavities. The two volumes considered are of size 1024×1004×551 voxels.

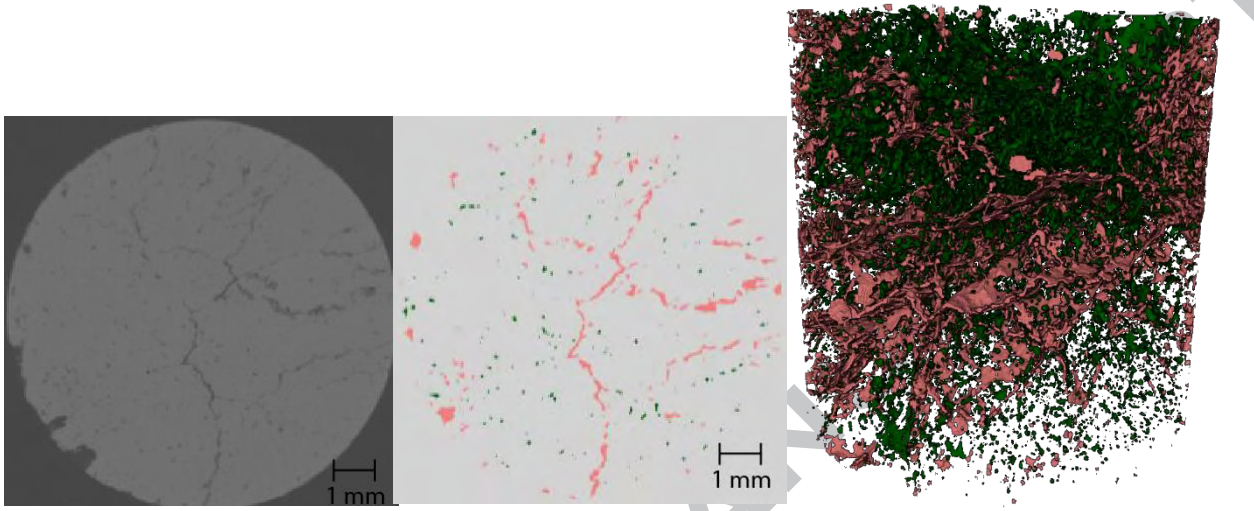

Figure 7a, b and c. Horizontally sliced plane and corresponding segmentation and 3D illustration for sample solidified with minimal supercooling.

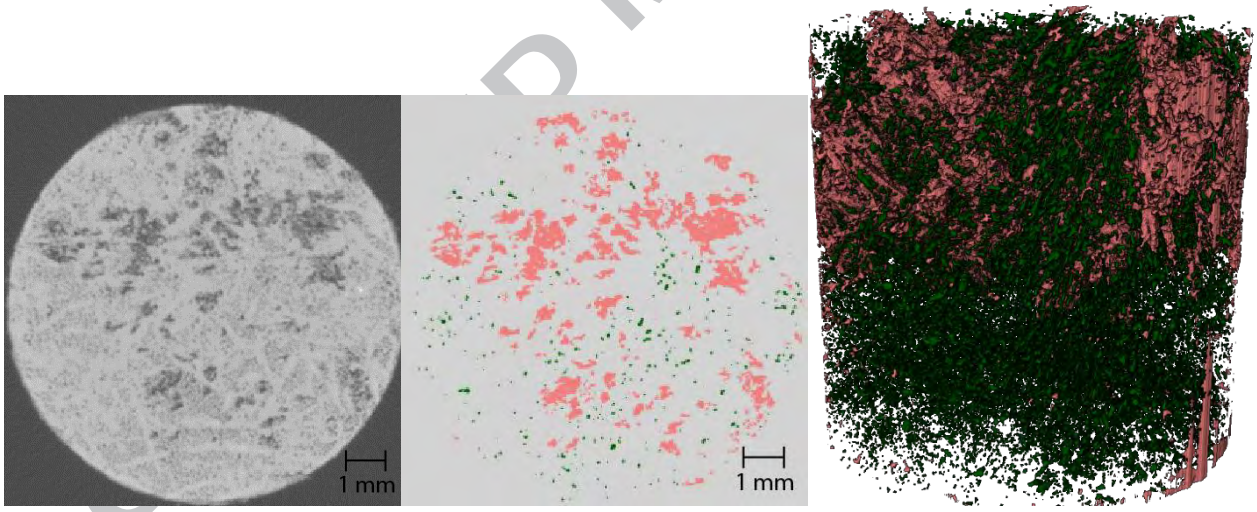

Figure 8a, b and c. Horizontally sliced plane and corresponding segmentation and 3D illustration for sample solidified with supercooling.

The fractions of air inside the samples are estimated based on the selected volumes, which represents a bulk of the samples. Based on the segmentation results, the air/cavity in the samples is determined. The fractions are listed in Table 1. The “cavity/total sample volume” fraction refers to the total volume of cavities related to the total sample volume. The “enclosed cavity/total cavity” gives the fraction of the cavity volume, which is enclosed related to the total cavity volume. In this context, enclosed cavities are fully surrounded by PCM whereas the non-enclosed cavities are interconnected. It shows that the total fraction of air/cavity in the sample, which had been supercooled, is as expected larger than in the sample where supercooling was avoided. This confirms the first hand impression of the samples. It can also be seen

that the amount of enclosed cavity with respect to the total cavity volume, is higher in the minimal degree supercooled sample.

Table 1. Total cavities and enclosed cavity

	Cavity/total sample volume	Enclosed cavity/total cavity
Non supercooled sample	0.07	0.13
Supercooled sample	0.15	0.09

4. Conclusions

The density of SAT crystalized from supercooled state and with minimal supercooling was measured to be 1.26 g/cm^3 and 1.34 g/cm^3 at 25 °C, which is significant lower than the literature value for solid SAT of 1.45 g/cm^3. This was due to cavities formed inside the SAT during the crystallization. The densities were slightly temperature dependent.

The density of liquid SAT was measured to be 1.29 g/cm^3 at 60 °C and 1.27 g/cm^3 at 90 °C. This fits well with the literature value for liquid SAT. The liquid density of SAT with extra water was proportional lower and was successfully measured in supercooled state down to 20 °C.

X-ray scanning and segmentation of solid SAT samples showed that a sample, which had solidified from supercooled state contained 15% air/cavity and a sample which had solidified with minimal supercooling contained 9% air/cavity. In both sample types the majority of the cavities were connected.

Temperature dependent expressions for the solid and liquid density of SAT derived from the measurements and the determined air/cavity fractions are summarized in Table 2.

Table 2. Results summary.

Sample	**Cavity/ total sample volume**	**Enclosed cavity/ total cavity**	**Density g/cm^3**
Solid SAT (non-supercooled)	0.07	0.13	$\rho_{s(non-supercool)} = -7.8 \cdot 10^{-5} \cdot T + 1.3423$ For 10 °C ≤ T ≤ 40 °C
Solid SAT (supercooled)	0.15	0.09	$\rho_{s(supercool)} = -7.6 \cdot 10^{-5} \cdot T + 1.2622$ For 10 °C ≤ T ≤ 50 °C.
Liquid SAT	NA	NA	$\rho_l = -7.5806 \cdot 10^{-4} \cdot T - 4.6340 \cdot 10^{-3} \cdot w + 1.5218$ For 20 °C ≤ T ≤ 80 °C, 44 % ≤ w ≤ 48 %; 30 °C ≤ T ≤ 80 °C, w = 42 % and 60 °C ≤ T ≤ 90 °C, w = 39.7 %.

Acknowledgements

Experimental investigations on density with TMA841 and DM40 were carried out in the laboratory of the GITSE research group, University of Zaragoza. Measurement of density of liquid SAT with extra water was carried out at Graz University of Technology. X-ray scanning was carried out at Department of Physics,

Technical University of Denmark. The authors thank the Spanish Ministry of Economy and Competitiveness for the funding of this work within the framework of projects ENE2011-28269-C03-01and ENE2014- 57262-R and the Danish Energy Agency supporting the joint IEA SHC Task 42/ ECES Annex 29 program on Compact Thermal Energy Storage, Grant no. 64012-0220.

[1] S.K. Sharma, C.K. Jotshi, S. Kumar, Thermal stability of sodium salt hydrates for solar energy storage applications, Sol. Energy. 45 (1990) 177–181. doi:10.1016/0038-092X(90)90051-D.

[2] L.F. Cabeza, G. Svensson, S. Hiebler, H. Mehling, Thermal performance of sodium acetate trihydrate thickened with different materials as phase change energy storage material, Appl. Therm. Eng. 23 (2003) 1697–1704. doi:10.1016/S1359-4311(03)00107-8.

[3] B. Zalba, J.M. Marín, L.F. Cabeza, H. Mehling, Review on thermal energy storage with phase change: materials, heat transfer analysis and applications, Appl. Therm. Eng. 23 (2003) 251–283. doi:10.1016/S1359-4311(02)00192-8.

[4] B. Sandnes, J. Rekstad, Supercooling salt hydrates: Stored enthalpy as a function of temperature, Sol. Energy. 80 (2006) 616–625. doi:10.1016/j.solener.2004.11.014.

[5] H. Kimura, J. Kai, Phase change stability of sodium acetate trihydrate and its mixtures, Sol. Energy. 35 (1985) 527–534. doi:10.1016/0038-092X(85)90121-5.

[6] T. Kousksou, P. Bruel, A. Jamil, T. El Rhafiki, Y. Zeraouli, Energy storage: Applications and challenges, Sol. Energy Mater. Sol. Cells. 120 (2014) 59–80. doi:10.1016/j.solmat.2013.08.015.

[7] A. Sharma, V. V. Tyagi, C.R. Chen, D. Buddhi, Review on thermal energy storage with phase change materials and applications, Renew. Sustain. Energy Rev. 13 (2009) 318–345. doi:10.1016/j.rser.2007.10.005.

[8] M. Dannemand, J.M. Schultz, J.B. Johansen, S. Furbo, Long term thermal energy storage with stable supercooled sodium acetate trihydrate, Appl. Therm. Eng. 91 (2015) 671–678. doi:10.1016/j.applthermaleng.2015.08.055.

[9] M. Kenisarin, K. Mahkamov, Salt hydrates as latent heat storage materials : Thermophysical properties and costs, Sol. Energy Mater. Sol. Cells. 145 (2016) 255–286. doi:10.1016/j.solmat.2015.10.029.

[10] P.B. Salunkhe, D. Jaya Krishna, Investigations on latent heat storage materials for solar water and space heating applications, J. Energy Storage. 12 (2017) 243–260. doi:10.1016/j.est.2017.05.008.

[11] P. Hu, D.-J. Lu, X.-Y. Fan, X. Zhou, Z.-S. Chen, Phase change performance of sodium acetate trihydrate with AlN nanoparticles and CMC, Sol. Energy Mater. Sol. Cells. 95 (2011) 2645–2649. doi:10.1016/j.solmat.2011.05.025.

[12] B.M.L. Garay Ramirez, C. Glorieux, E.S. Martin Martinez, J.J.A. Flores Cuautle, Tuning of thermal properties of sodium acetate trihydrate by blending with polymer and silver nanoparticles, Appl. Therm. Eng. 61 (2013) 838–844. doi:10.1016/j.applthermaleng.2013.09.049.

[13] X. Li, Y. Zhou, H. Nian, F. Zhu, X. Ren, O. Dong, C. Hai, Y. Shen, J. Zeng, Preparation and thermal energy storage studies of CH3COONa·3H2O-KCl composites salt system with enhanced phase change performance, Appl. Therm. Eng. 102 (2016) 708–715. doi:10.1016/j.applthermaleng.2016.04.029.

[14] J. Mao, P. Hou, R. Liu, F. Chen, X. Dong, Preparation and thermal properties of SAT-CMC-DSP/EG composite as phase change material, Appl. Therm. Eng. 119 (2017) 585–592. doi:10.1016/j.applthermaleng.2017.03.097.

[15] M. Jinfeng, D. Xian, H. Pumin, L. Huiliang, Preparation research of novel composite phase change materials based on sodium acetate trihydrate, Appl. Therm. Eng. 118 (2017) 817–825. doi:10.1016/j.applthermaleng.2017.02.102.

[16] M. Dannemand, J. Dragsted, J. Fan, J.B. Johansen, W. Kong, S. Furbo, Experimental investigations on prototype heat storage units utilizing stable supercooling of sodium acetate trihydrate mixtures, Appl. Energy. 169 (2016) 72–80. doi:10.1016/j.apenergy.2016.02.038.

[17] M. Dannemand, J.B. Johansen, W. Kong, S. Furbo, Experimental investigations on cylindrical latent heat storage units with sodium acetate trihydrate composites utilizing supercooling, Appl. Energy. 177 (2016) 591–601. doi:10.1016/j.apenergy.2016.05.144.

[18] A. Safari, R. Saidur, F.A. Sulaiman, Y. Xu, J. Dong, A review on supercooling of Phase Change Materials in thermal energy storage systems, Renew. Sustain. Energy Rev. (2016) 1–15. doi:10.1016/j.rser.2016.11.272.

[19] M. Dannemand, J.B. Johansen, S. Furbo, Solidification Behavior and Thermal Conductivity of Bulk Sodium Acetate Trihydrate Composites with Thickening Agents and Graphite, Sol. Energy Mater. Sol. Cells. 145 (2016) 287–295. doi:10.1016/j.solmat.2015.10.038.

[20] W. Kong, M. Dannemand, J.B. Johansen, J. Fan, J. Dragsted, G. Englmair, S. Furbo, Experimental investigations on heat content of supercooled sodium acetate trihydrate by a simple heat loss method, Sol. Energy. 139 (2016) 249–257. doi:10.1016/j.solener.2016.09.045.

[21] Z. Ma, H. Bao, A.P. Roskilly, Study on solidification process of sodium acetate trihydrate for seasonal solar thermal energy storage, Sol. Energy Mater. Sol. Cells. 172 (2017) 99–107. doi:10.1016/j.solmat.2017.07.024.

[22] L.F. Cabeza, A. Castell, C. Barreneche, A. de Gracia, A.I. Fernández, Materials used as PCM in thermal energy storage in buildings: A review, Renew. Sustain. Energy Rev. 15 (2011) 1675–1695. doi:10.1016/j.rser.2010.11.018.

[23] H. Inaba, H. Otake, S. Nozo, T. Fukuda, A study on latent heat storage using a supercooled condition of hydrate (1st report, an estimation of Physical properties of hydrate sodium acetate including a supercooling condition), Japan Soc. Mech. Eng. 553 (1992) 2848–2856. doi:10.1299/kikaib.58.2848.

[24] Z. Khan, Z. Khan, A. Ghafoor, A review of performance enhancement of PCM based latent heat storage system within the context of materials, thermal stability and compatibility, Energy Convers. Manag. 115 (2016) 132–158. doi:10.1016/j.enconman.2016.02.045.

[25] G.R. Dheep, A. Sreekumar, Influence of nanomaterials on properties of latent heat solar thermal energy storage materials – A review, Energy Convers. Manag. 83 (2014) 133–148. doi:10.1016/j.enconman.2014.03.058.

[26] M.K.A. Sharif, A.A. Al-Abidi, S. Mat, K. Sopian, M.H. Ruslan, M.Y. Sulaiman, R. M.A.M., Review of the application of phase change material for heating and domestic hot water systems, Renew. Sustain. Energy Rev. 42 (2015) 557–568. doi:10.1016/j.rser.2014.09.034.

[27] J. Xu, R.Z. Wang, Y. Li, A review of available technologies for seasonal thermal energy storage, Sol.

Energy. 103 (2013) 610–638. doi:10.1016/j.solener.2013.06.006.

[28] G. Zhou, Y. Han, Numerical simulation on thermal characteristics of supercooled salt hydrate PCM for energy storage: Multiphase model, Appl. Therm. Eng. 125 (2017) 145–152. doi:10.1016/j.applthermaleng.2017.07.010.

[29] D. Aydin, Z. Utlu, O. Kincay, Thermal performance analysis of a solar energy sourced latent heat storage, Renew. Sustain. Energy Rev. 50 (2015) 1213–1225. doi:10.1016/j.rser.2015.04.195.

[30] M.A. Fazilati, A.A. Alemrajabi, Phase change material for enhancing solar water heater, an experimental approach, Energy Convers. Manag. 71 (2013) 138–145. doi:10.1016/j.enconman.2013.03.034.

[31] W. Streicher, Final report of Subtask C “Phase Change Materials”. The overview. A report from IEA Solar heating and Cooling Programme Task 32 Advanced Storage Concepts for solar and low energy buildings, (2008).

[32] M. Rommel, A. Hauer, W. Van Helden, Compact Thermal Energy Storage IEA SHC Position Paper, 2015.

[33] S. Furbo, HEAT STORAGE WITH AN INCOIIGRUENTLY MELTING SALT HYDRATE AS STORAGE MEDIUM BASED ON THE EXTRA WATER PRINCIPLE, Thermal Insulation Laboratory, Technical University of Denmark, Report no. 108, Kgs. Lyngby, Denmark, 1980.

[34] S. Furbo, Investigations of Heat Storages with salt hydrate as storage medium based on the extra water principle, Therm. Insul. Lab. DTU, Kgs. Lyngby, Denmark, Rep. 80. Meddelelse (1978).

[35] A. Kaizawa, H. Kamano, A. Kawai, T. Jozuka, T. Senda, N. Maruoka, T. Akiyama, Thermal and flow behaviors in heat transportation container using phase change material, Energy Convers. Manag. 49 (2008) 698–706. doi:10.1016/j.enconman.2007.07.022.

[36] H.G. Yücel, Prediction of molecular weight and density of n-alkanes (C6-C44), Anal. Chim. Acta. 547 (2005) 94–97. doi:10.1016/j.aca.2005.01.072.

[37] L.A. Feldkamp, L.C. Davis, J.W. Kress, Practical cone-beam algorithm, J. Opt. Soc. Am. A. 1 (1984) 612. doi:10.1364/JOSAA.1.000612.

[38] G.A. Lane, Solar heat storage latent heat material Vol 1, CRC, Boca Raton, Florida, United states, 1983.

Highlights:

- Density of liquid and solid sodium acetate trihydrate (SAT) was measured
- Density of supercooled SAT with extra water was measured
- Solidified SAT contained cavities
- Cavity fraction in solid SAT depended on solidification
- The density of SAT was lower after solidified with a high degree of supercooling

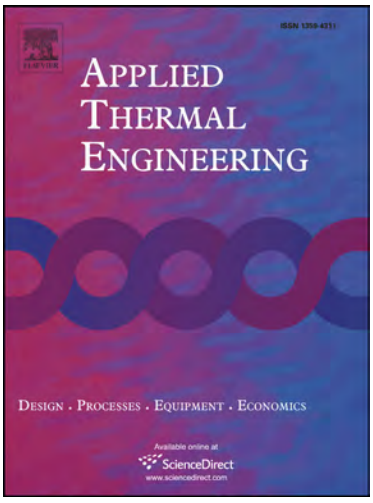

Porosity and density measurements of sodium acetate trihydrate for thermal energy storage

Mark Dannemand, Monica Delgado, Ana Lazaro, Conchita Peñalosa, Carsten Gundlach, Camilla Trinderup, Jakob Berg Johansen, Christoph Moser, Hermann Schranszhofer, Simon Furbo

PII: S1359-4311(17)34932-3
DOI: https://doi.org/10.1016/j.applthermaleng.2017.12.052
Reference: ATE 11573

To appear in: *Applied Thermal Engineering*

Received Date: 26 July 2017
Revised Date: 15 October 2017
Accepted Date: 11 December 2017

Please cite this article as: M. Dannemand, M. Delgado, A. Lazaro, C. Peñalosa, C. Gundlach, C. Trinderup, J. Berg Johansen, C. Moser, H. Schranszhofer, S. Furbo, Porosity and density measurements of sodium acetate trihydrate for thermal energy storage, *Applied Thermal Engineering* (2017), doi: https://doi.org/10.1016/j.applthermaleng.2017.12.052